NASA Technical Memorandum 104381
ICOMP-91-8

# Microfracture in High Temperature Metal Matrix Crossply Laminates



Subodh K. Mital
*Institute for Computational Mechanics in Propulsion*
*Lewis Research Center*
*Cleveland, Ohio*

and

Christos C. Chamis
*Lewis Research Center*
*Cleveland, Ohio*

Prepared for the
Winter Annual Meeting and Symposium on Failure Mechanisms
in High Temperature Composites
sponsored by the American Society of Mechanical Engineers
Atlanta, Georgia, December 1-6, 1991

NASA

# MICROFRACTURE IN HIGH TEMPERATURE METAL MATRIX CROSSPLY LAMINATES

Subodh K. Mital*
Institute for Computational Mechanics in Propulsion
Lewis Research Center
Cleveland, Ohio 44135

and

Christos C. Chamis
National Aeronautics and Space Administration
Lewis Research Center
Cleveland, Ohio 44135



## ABSTRACT

Microfracture (fiber/matrix fracture, interphase debonding and inter-ply delamination) in high temperature metal matrix composites (HTMMC), subjected to both mechanical and thermal loading, is computationally simulated. A crossply 0.3 fiber volume ratio SiC/Ti15 composite with 0/90/0 lay-up is evaluated for microfracture using a multicell finite element model. A computational simulation procedure based on strain energy release rates is used to predict the fracture process and establish the hierarchy of fracture modes. Microfracture results for various loading cases are presented and discussed.

## INTRODUCTION

Microfracture, defined as fiber or matrix fracture, fiber-matrix interface debonding or delamination through the inter-ply layer, is critical in assessing structural integrity and durability. Traditionally, researchers looked at the microfracture using stresses, strains and stress intensity factors at the local level for the crack initiation and propagation. An alternate approach is to assess the effect of microfracture on the global response.

In previous works (1,2), microfracture was computationally simulated for a unidirectional metal matrix composite subjected to various types of mechanical and thermal loads. Microfracture propagation and the extent of stress redistribution in the surrounding fiber and matrix due to fiber/matrix fracture, interface debonding and inter-ply delamination, were computationally simulated for a unidirectional metal matrix composite. A computational simulation procedure based on three-dimensional finite element analysis and global strain energy release rates was developed to predict the microfracture process and identify/quantify the hierarchy of respective fracture modes under various types of loading. Step-by-step procedures were outlined to evaluate composite microfracture and establish the hierarchy of respective fracture modes for a given composite system. The procedure was applied on a unidirectional SiC/Ti15 composite with a fiber volume ratio of 0.35. Typical results indicate that if the composite is subjected to longitudinal (along the fiber) loading, interphase debonding is not likely to initiate by itself, it will only occur if it is preceded by fiber or matrix fracture. This demonstrates that debonding is a

*Work funded by Space Act Agreement C99066 G.

weaker fracture mode and is likely to instantaneously follow the stronger fracture modes (fiber/matrix fracture) when the composite is subjected to longitudinal tensile loads (1). It also showed that microfracture propagation is rather insensitive to thermal loads alone. Microfracture was also simulated for other types of mechanical loading. A similar type of procedure has been applied very successfully to simulate a fiber pushout test (3).

The objective of the present paper is to evaluate microfracture and identify/quantify the microfracture modes and propagation for a crossply metal matrix composite subjected to thermo-mechanical loads.

## FINITE ELEMENT MODEL

The finite element model used in the computational simulation procedure consists of a group of nine fibers in a three-by-three unit cell array. The composite system has three plies with 0/90/0 lay-up and consists of 30 percent fiber volume ratio (fvr) SiC/Ti15 metal matrix composite (silicon carbide fiber and titanium alloy matrix). There are six elements ("bays") along the length of the fiber. Each unit cell as shown in Fig. 1, consists of 40 hexahedron (six-sided) and 8 pentahedron (five-sided) solid elements for a total of 2952 elements and 2863 nodes in the model. The properties of the constituents at the reference (room) temperature are shown in Table I. The interphase properties are assumed to be the same as matrix properties in this work.

In a typical set of simulations, fracture is initiated in the fiber at the middle of the center cell and is allowed to propagate either through the matrix or along the fiber-matrix interface. In the debonding mode, fracture is introduced around the fiber, such that the whole fiber circumference is debonded. Similarly, the crack could be initiated in the matrix or the fiber-matrix interface. Fracture is simulated by placing duplicate node points on either side of the crack. These duplicate nodal or grid points have the same geometrical location, but no connectivity exists between them, thus, in effect producing a crack of zero width. For a given fracture configuration, either uniform boundary displacements in case of mechanical loading or nodal temperatures in case of thermal loads are specified. Resulting nodal forces, computed from finite element analysis are compared for reduction in global stiffness and strain energy release rates are computed. In the case of thermal loading, strain energy release rates computed are based on total strain energy of all elements, as will be explained below. Complete details of the procedure are described in Refs. 1 and 2.

## STRAIN ENERGY RELEASE RATE

Strain energy release rate (SERR) is an acceptable indicator of the fracture toughness of a material. It gives a measure of the amount of energy required to propagate a defect in a material. Hence, one can make a direct comparison of damage tolerances between different microfracture configurations (modes/paths), materials and geometries. In the present research, a global approach has been used to calculate strain energy release rate. In this approach, applied nodal displacements and corresponding nodal forces are used to calculate the work done. Strain energy release rate, G, is then, calculated as:

$$G = \frac{dW}{dA} = \frac{1}{2} \bullet \frac{(F_2 - F_1) \bullet u}{\Delta A} \qquad (1)$$

| | |
|---|---|
| $dW$ | change in work done |
| $\Delta A$ | area of the new surfaces generated |
| $u$ | applied displacement at the loaded end of the model |
| $F_1$, $F_2$ | forces at the end nodes before and after $\Delta A$, respectively |

The above equation is simply the incremental change in work divided by the incremental change in new surface area that opens up from one fracture configuration to the other. The applied displacement between two fracture configurations is kept the same, while the nodal forces required to maintain that displacement change because of the reduction in global stiffness as the fracture propagates. Using this approach, one can calculate the reduction in global stiffness as the crack propagates as well as compare the SERR for different fracture configurations.

In the case of thermal loading, strain energy release rates are calculated by comparing total strain energies of different fracture configurations. Strain energy release rate is then, calculated as :

$$G = \frac{dW}{dA} = \frac{1}{2} \bullet \frac{(S.E.)_2 - (S.E.)_1}{\Delta A} \qquad (2)$$

$(S.E.)_1$, $(S.E.)_2$: strain energy in the fracture configuration 1 and 2, respectively.

The advantage of using a global (total) strain energy release rate formulation is that it bypasses local stress details like stress gradients that usually cause convergence problems. One other method, used to calculate strain energy release is the crack closure method. This is a local level approach since the nodal displacements and the corresponding nodal forces at the crack tip location are used to calculate the amount of work required to close the crack, which has been extended by an incremental amount. For the case of thermal loading, SERR were computed by using both the crack closure method and the total strain energy formulation. Both methods give same results, although, using the total strain energy formulation is computationally more effective and elegant. One can use the crack closure method if one is interested in identifying each mode of failure. In the present work, the total strain energy formulation for computing SERR is used in the case of thermal loading.

## CASES STUDIED AND RESULTS

### 1-1 and 2-2 Direction Loading

For this loading case, fracture was initiated in the middle of the center cell fiber and then propagated in the matrix or the fiber-matrix interface. 1-1 and 2-2 direction loadings have shown essentially the same microfracture behavior. If a fiber is fractured in a ply which is oriented in the loading direction, its microfracture behavior is the same as that observed in the unidirectional composite reported earlier (1). If a fiber is fractured, interphase debonding is likely to follow instantaneously. For example, if the composite is loaded in the 2-2 direction, there is about a 10 percent reduction in global stiffness in the 2-2 direction when the center fiber is fully debonded as shown in Fig. 2(a). The corresponding strain energy release rate curve is shown in Fig. 2(b). If the fracture was initiated and propagated in the fiber-matrix interface, there was no

reduction in the global stiffness and hence the SERR was also zero. Thus, it can be concluded that debonding does not initiate by itself, it occurs following the fiber or matrix fracture. The propagation of the fracture depends upon the relative fracture toughness of the constituent materials. But, it has been observed that the stress concentration at the crack tip in this composite for different types of loads is much less than what would be expected in a homogeneous material. Hence, the crack propagation will be governed by the tensile strength of the fiber and matrix, and the shear strength of the interphase material.

If the fracture initiates in the matrix, it propagates through the matrix in the neighboring plies. When the fracture hits the fiber in the neighboring ply, which is oriented perpendicular to the loading direction, the crack, then, propagates through the interphase. There is about 11 percent reduction in global stiffness for a fully debonded fiber as shown in Fig. 3(a) and the corresponding strain energy release rate is shown in Fig. 3(b).

3-3 Direction Loading

When the composite is loaded in the 3-3 direction, there is no reduction in global stiffness in the 3-3 direction due to a fiber fracture only. However, if the fracture initiates in the matrix and propagates in the interphase, there is a gradual decrease in global stiffness in the 3-3 direction. When 70 percent of the total fiber surface area is debonded, there is about 50 percent reduction in global stiffness in the 3-3 direction as shown in Fig. 4(a). The corresponding strain energy release rate curve is shown in Fig. 4(b). The fracture propagation in this mode seems to be stable as the additional energy needed to drive the crack reduces. However, it was observed for a unidirectional composite under transverse loading that once about 10 percent of the fiber surface area is debonded, it takes much less energy to drive the crack further (1), indicating crack propagation instability and high sensitivity of debonding extension due to transverse loading.

1-2 and 1-3 Shear Loading

Shear loading was applied to the specimen in both 1-2 and 1-3 directions. Results of both of these shear loadings are similar. If only a fiber or the matrix is fractured, it does not reduce the global stiffness and thus, the corresponding strain energy release rates are also negligible. However, there is a gradual decrease in stiffness as fibers start to debond (Fig. 5(a)). There is about 7 percent reduction in stiffness for the fully debonded center cell fiber. The corresponding strain energy release rate is shown in Fig. 5(b). Fracture propagation in this loading case is stable as the additional energy needed to drive the crack reduces as the fracture propagates. For the crossply composite subjected to 3-3 (thru-the thickness) or the shear loads, fiber-matrix interface debonding is the only mode of fracture propagation. However, thru-the-thickness (3-3) loading is much more indicative of interfacial conditions than the shear loading.

Thermal Loading

Various thermal loading cases were evaluated for microfracture propagation for this composite. Results for two typical loading cases are presented here. In the first loading case, the composite was uniformly heated from room temperature to a temperature of 300 °C (570 °F) i.e., $\Delta T$ of 500 °F. Constituent properties at room temperature as shown in Table I are used and assumed to remain constant for the above thermal loading case. Fracture is initiated in the matrix and interphase region. Various fracture configurations were evaluated for this loading case and the strain energy release rate was computed using Eq. (2) by comparing total strain-energies in different microfracture configurations. When the center cell fiber is

fully debonded, the change in total strain energy from reference (no fracture) state to this fracture configuration is only 0.4 percent and thus, the strain energy release rate is also negligibly small. The strain energy release rates for other fracture configurations for this loading case are also very small. Hence, it can be concluded that microfracture propagation is quite insensitive to temperature increases up to 260 °C (500 °F) from room temperature.

In the next set of simulations, the composite is cooled down from 815 to -185 °C, i.e., $\Delta T$ of 1000 °C (1800 °F). The constituent properties at higher temperature are computed by using a "mutlifactor interaction equation (MFIE)" (4,5). This equation proposes modeling the material behavior using a time-temperature-stress dependence of constituent's properties in a "material behavior space," as follows:

$$\frac{P}{P_o} = \left[\frac{T_F - T}{T_F - T_o}\right]^n \cdot \left[\frac{S_F - \sigma}{S_F - \sigma_o}\right]^m \cdots \tag{3}$$

where

| | |
|---|---|
| P | property |
| T | temperature |
| S | strength |
| $\sigma$ | stress |
| 0 | reference |
| F | final |
| m,n | exponents |

It assumes that various factors such as temperature, stress, stress rate etc. influence the in-situ constituent material behavior. The multifactor interaction Eq. (3) represents gradual effects during most ranges and rapidly degrading properties near the final stages as has been observed experimentally. The exponents are determined from experimental data, wherever possible, otherwise default values are used which were established from studies conducted on other materials.

In the present work, in-situ constituent properties are assumed to depend only on temperature (m = 0). The value of the exponent n is taken 0.5 for the matrix and 0.25 for the fiber. The final temperature is assumed to be the melting temperature of the constituent and the reference temperature is taken as the room temperature. Constituent properties at 815 °C, calculated using equation (3) are shown in Table II, are assumed to remain constant for this loading case. For this composite $\alpha_f < \alpha_m$, so when the composite is cooled down, there are tensile stresses in the matrix while the fiber stresses are compressive. Hence, the fracture is likely to initiate in the matrix or the interphase. Thus, the fracture was initiated in the matrix because of the stress state in the composite, and propagated through the matrix or the interphase. Fracture was also propagated in the inter-ply region to delaminate the top and middle plies. When the fracture propagates in the interphase region following the matrix fracture, SERR is very small and is shown in Fig. 6. Hence, the crossply composite will show some amount of debonding and will show ductile behavior under this type of thermal loading.

## CONCLUSIONS

A computational simulation procedure, proposed for microfracture evaluation of HTMMC subjected to mechanical and thermal loadings, is applied to a crossply laminate. The significant results from this work are as follows:

1. When the composite is subjected to 1-1 or 2-2 loading, then a fiber fracture in a ply which is oriented in the loading direction, will likely be instantaneously followed by interphase debonding. Interphase debonding will not initiate by itself, the same behavior that was observed for a unidirectional composite. If the fracture initiates in the matrix, it propagates through the matrix to the neighboring plies and then propagates along the fiber-matrix interface.

2. When the composite is loaded in the 3-3 direction, debonding along the fiber-matrix interface is the only mode for fracture propagation.

3. For composites subjected to shear loads, fiber-matrix interface debonding is the only likely mode for fracture propagation. However, the composite is not as sensitive to debonding extension under shear load as it is under thru-the-thickness (3-3) load.

4. In general, microfracture propagation in crossply metal matrix composites under thermal loads alone is not as sensitive as it is under mechanical loads.

5. Microfracture propagation is not sensitive for a temperature increase of 260 °C/500 °F from room temperature. If the composite is cooled down from high temperature to cryogenic temperature, the fracture will likely propagate through the fiber-matrix interface, thus showing higher apparent fracture toughness.

## REFERENCES


1. Mital, S.K., Caruso, J.J., and Chamis, C.C., 1990, "Metal Matrix Composites Microfracture: Computational Simulation," Computers & Structures, Vol. 37, No. 2, pp. 141-150 (Also, NASA TM-103153).

2. Mital, S.K. and Chamis C.C., "Thermally-Driven Microfracture in High Temperature Metal Matrix Composites," to appear in the Proceedings of the Symposium on the Mechanics of Composites at Elevated and Cryogenic Temperatures, ASME Applied Mechanics Division Meeting, Columbus, OH, June 16-19, 1991.

3. Mital, S.K. and Chamis, C.C., 1990, "Fiber Pushout Test: A Three-Dimensional Finite Element Computational Simulation," ASTM Journal of Composites Technology and Research, Vol. 13, No. 1, pp. 14-21 (Also NASA TM-102565).

4. Hopkins, D.A. and Chamis, C.C., 1985, "A Unique Set of Micromechanics Equations for High Temperature Metal Matrix Composites," NASA TM-87154.

5. Murthy, P.L.N., Hopkins, D.A., and Chamis, C.C., 1989, Metal Matrix Composite Micromechanics: In-Situ Behavior Influence on Composite Properties. NASA TM-102302.

TABLE I. - PROPERTIES OF CONSTITUENT MATERIALS

OF SiC/Ti15 at 21 °C

[1 GPa = 1000 MPa; 1 MPa = 145 psi.]

| | SiC fiber | Ti15 matrix | Interphase |
|---|---|---|---|
| Modulus, E (GPa) | 428 | 85 | 85 |
| Poisson's ratio, $\nu$ | 0.3 | 0.32 | 0.32 |
| Shear modulus, G (GPa) | 164 | 32 | 32 |
| Coefficient of thermal expansion, $\alpha$ (ppm/°C) | 3.2 | 8.1 | 8.1 |

TABLE II. - PROPERTIES OF CONSTITUENT MATERIALS

OF SiC/Ti15 at 815 °C

| | SiC fiber | Ti15 matrix | Interphase |
|---|---|---|---|
| Modulus, E (GPa) | 393 | 46 | 46 |
| Poisson's ratio, $\nu$ | 0.27 | 0.15 | 0.15 |
| Shear modulus, G (GPa) | 153 | 19.6 | 19.6 |
| Coefficient of thermal expansion, $\alpha$ (ppm/°C) | 3.5 | 23.0 | 23.0 |

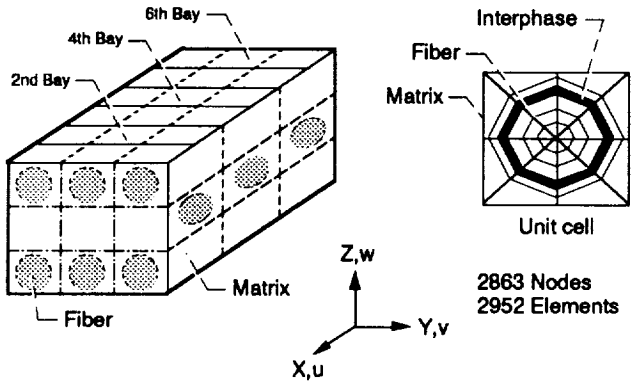


Figure 1.—Schematic diagram of cross-plied (0/90/0) model.

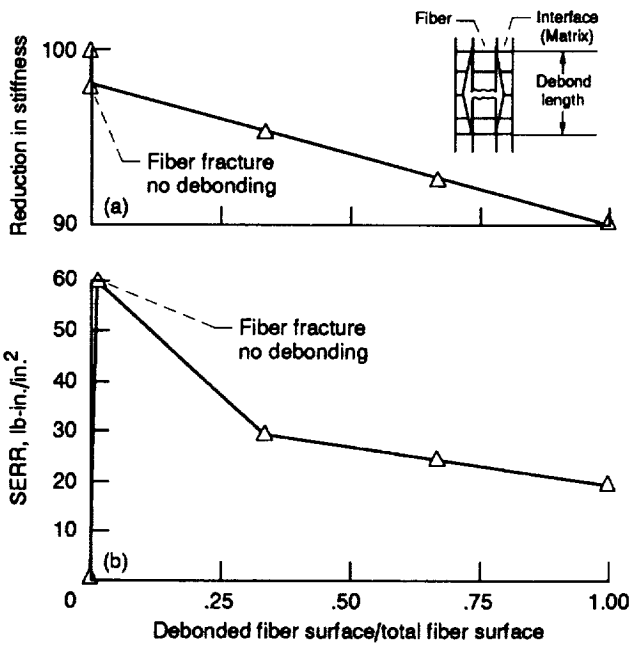


Figure 2.—Stiffness reduction and strain energy release rate for center cell fiber debonding; fiber initiated crack under 2-2 load.

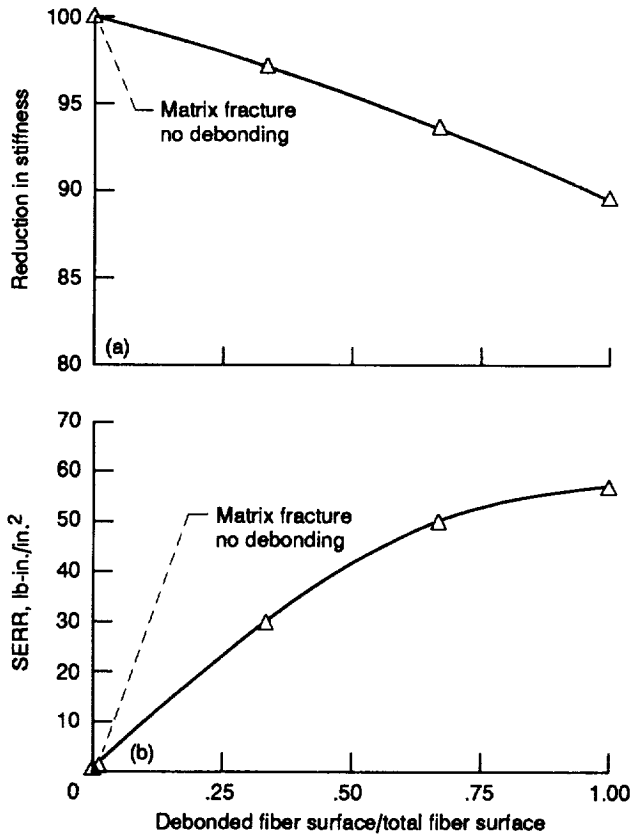


Figure 3.—Stiffness reduction and strain energy release rate for one fiber debonding; matrix initiated crack under 2-2 load.

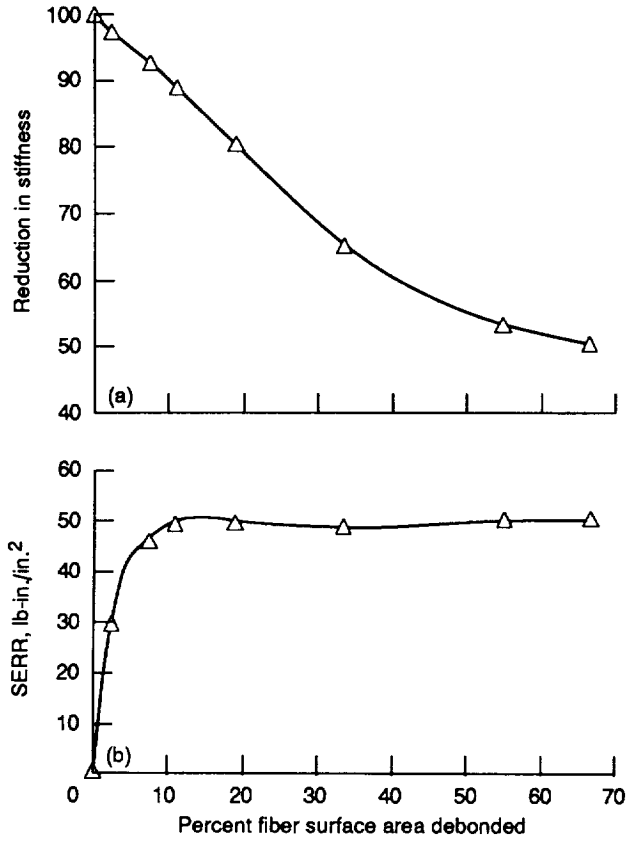


Figure 4.—Stiffness reduction and strain energy release rate versus percent fiber surface debonded; 3-3 load.

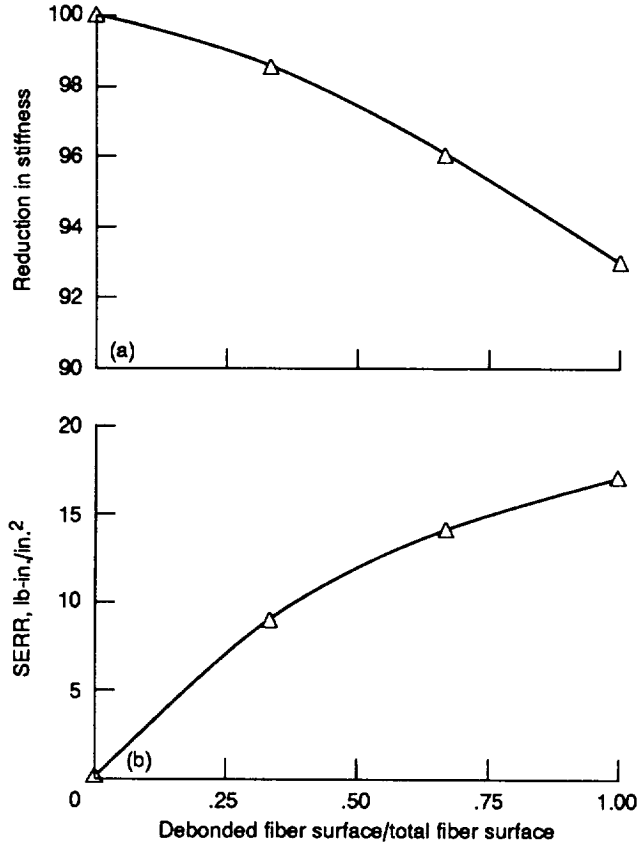


Figure 5.—Reduction in stiffness and strain energy release rate for center cell fiber debonding; 1-2 shear load.

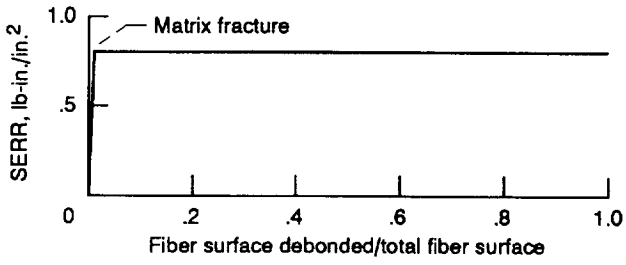


Figure 6.—SERR for center fiber debonding; uniform cooling (815 to −185 °C).

NASA
National Aeronautics and Space Administration

# Report Documentation Page

| 1. Report No. | 2. Government Accession No. | 3. Recipient's Catalog No. |
|---|---|---|
| NASA TM -104381<br>ICOMP-91-8 | | |

**4. Title and Subtitle**
Microfracture in High Temperature Metal Matrix Crossply Laminates

**5. Report Date**

**6. Performing Organization Code**

**7. Author(s)**
Subodh K. Mital and Christos C. Chamis

**8. Performing Organization Report No.**
E -6201

**10. Work Unit No.**
510-10-50

**9. Performing Organization Name and Address**
National Aeronautics and Space Administration
Lewis Research Center
Cleveland, Ohio 44135 - 3191

**11. Contract or Grant No.**

**13. Type of Report and Period Covered**
Technical Memorandum

**12. Sponsoring Agency Name and Address**
National Aeronautics and Space Administration
Washington, D.C. 20546 - 0001

**14. Sponsoring Agency Code**

**15. Supplementary Notes**
Prepared for the Winter Annual Meeting and Symposium on Failure Mechanisms in High Temperature Composites sponsored by the American Society of Mechanical Engineers, Atlanta, Georgia, December 1-6, 1991. Subodh K. Mital, Institute for Computational Mechanics in Propulsion, NASA Lewis Research Center (work funded under Space Act Agreement C990669), Space Act Monitor; Louis A. Povinelli (216) 433-5818.

**16. Abstract**
Microfracture (fiber/matrix fracture, interphase debonding and inter-ply delamination) in high temperature metal matrix composites (HTMMC), subjected to both mechanical and thermal loading, is computationally simulated. A crossply 0.3 fiber volume ratio SiC/Ti15 composite with 0/90/0 lay-up is evaluated for microfracture using a multicell finite element model. A computational simulation procedure based on strain energy release rates is used to predict the fracture process and establish the hierarchy of fracture modes. Microfracture results for various loading cases are presented and discussed.

| 17. Key Words (Suggested by Author(s)) | 18. Distribution Statement |
|---|---|
| Composite materials; Metal matrix composite; Microfracture; Debonding; Interface; Interphase; Matrix fracture; Fiber fracture; Strain energy release rate | Unclassified - Unlimited<br>Subject Category 24 |

| 19. Security Classif. (of the report) | 20. Security Classif. (of this page) | 21. No. of pages | 22. Price* |
|---|---|---|---|
| Unclassified | Unclassified | 12 | A03 |

NASA FORM 1626 OCT 86

*For sale by the National Technical Information Service, Springfield, Virginia 22161